

Original article

Numerical simulation of two-phase flow in deformable porous media: Application to carbon dioxide storage in the subsurface

O. Kolditz^{a,b,*}, S. Bauer^g, N. Böttcher^c, D. Elsworth^f, U.-J. Görke^a,
C.-I. McDermott^e, C.-H. Park^{a,d}, A.K. Singh^a, J. Taron^{a,f}, W. Wang^a

^a Department of Environmental Informatics, Helmholtz Centre for Environmental Research – UFZ Leipzig, Germany

^b Environmental System Analysis, TU Dresden, Germany

^c Groundwater Management, TU Dresden, Germany

^d Department of Geothermal Resources, Korea Institute of Geoscience and Mineral Resources (KIGAM), Republic of Korea

^e School of Geosciences, Edinburgh University, UK

^f Center for Geomechanics, Geofluids and Geohazards, PennState, USA

^g Geohydromodelling, University of Kiel, Germany

Received 16 November 2009; received in revised form 24 June 2012; accepted 25 June 2012

Available online 6 July 2012

Abstract

In this paper, conceptual modeling as well as numerical simulation of two-phase flow in deep, deformable geological formations induced by CO₂ injection are presented. The conceptual approach is based on balance equations for mass, momentum and energy completed by appropriate constitutive relations for the fluid phases as well as the solid matrix. Within the context of the primary effects under consideration, the fluid motion will be expressed by the extended Darcy's law for two phase flow. Additionally, constraint conditions for the partial saturations and the pressure fractions of carbon dioxide and brine are defined. To characterize the stress state in the solid matrix, the effective stress principle is applied. Furthermore, the interaction of fluid and solid phases is illustrated by constitutive models for capillary pressure, porosity and permeability as functions of saturation. Based on this conceptual model, a coupled system of nonlinear differential equations for two-phase flow in a deformable porous matrix (H²M model) is formulated. As the displacement vector acts as primary variable for the solid matrix, multiphase flow is simulated using both pressure/pressure or pressure/saturation formulations. An object-oriented finite element method is used to solve the multi-field problem numerically. The capabilities of the model and the numerical tools to treat complex processes during CO₂ sequestration are demonstrated on three benchmark examples: (1) a 1-D case to investigate the influence of variable fluid properties, (2) 2-D vertical axi-symmetric cross-section to study the interaction between hydraulic and deformation processes, and (3) 3-D to test the stability and computational costs of the H²M model for real applications.

© 2012 IMACS. Published by Elsevier B.V. All rights reserved.

Keywords: Porous media; Two-phase flow consolidation; Heat transport; Carbon capture storage (CCS); OpenGeoSys (OGS)

1. Introduction

For about two decades, most of the earth's inhabitants have been experiencing increase in the average temperature in their living environment. Although there are different opinions, most of environmental scientists believe that global

* Corresponding author at: Department of Environmental Informatics, Helmholtz Centre for Environmental Research – UFZ Leipzig, TU Dresden, Germany.

E-mail address: olaf.kolditz@ufz.de (O. Kolditz).

warming is coming and people must take actions against it. The causes of the recent warming become an active field of research. Some scientists suppose that the human activity induced green house effect is the main reason of the global warming. A further study shows that on Earth the major greenhouse gases are water vapor, which causes about 36–70% of the greenhouse effect (not including clouds); carbon dioxide (CO₂), which causes 9–26%; methane (CH₄), which causes 4–9%; and ozone, which causes 3–7%, see Metz et al. [39]. Among the major greenhouse gases, CO₂ is the one that can be increased by human activities such as electricity generation. To reduce anthropogenic greenhouse gas emissions into the atmosphere, the carbon dioxide capture and storage (CCS) concept is considered as an emerging transition technology. The study of CCS is therefore under active consideration recently.

In 2005, the Intergovernmental Panel on Climate Change (IPCC) published a special report by Metz et al. [39] addressing the state-of-the-art, the perspectives and various knowledge gaps related to the long-term storage (sequestration) of CO₂ in subsurface. Three types of geological formations are particularly considered for the safe storage of CO₂: (nearly) depleted hydrocarbon reservoirs, deep saline aquifers and non-minable coal seams. In cases of hydrocarbon reservoirs and deep aquifers, carbon dioxide is injected in a dense form into porous rock formations filling out the pore space and partially displacing in situ residing fluids. According to various studies, deep saline aquifers provide the most substantial carbon dioxide storage capacity, see e.g. Förster et al. [20] and Arts et al. [1], and are often located near possible CO₂ sources such as coal-fired power plants.

To ascertain migration and trapping of CO₂ in the formations and assess the capacity and the safety (possible leakage) of the reservoir, the numerical simulation of injection and spreading of carbon dioxide in the underground is essential for understanding the physical and chemical processes at different length and time scales (see [9,14,26]). Existing numerical studies of carbon dioxide storage are mostly based on simulators developed for the use in the oil, gas and geothermal energy production. They represent convenient starting points for specialized models and code adaptations targeted at modeling the geological storage of CO₂, see Tsang [55], Pruess and Garcia [45] and Bielinski [8].

The injection of supercritical CO₂ into deep saline aquifers results in high pressure in the vicinity of the injection well, see Dentz and Tartakovsky [17] and Doughty and Pruess [18]. Due to the high injection pressure, the stress distribution in this reservoir region can be changed significantly. High pressure induced medium deformation must be considered to guarantee the safety assessment of the injection process. In the present study, we utilize numerical methods to analyze the stress changes caused by the interaction with the two phase fluids during the injection. To this purpose, we first set a conceptual injection model, which represents the two-phase fluid flow process of CO₂ and water, and also the deformation process in the near field in deep saline aquifers. To enable a stable and efficient simulation, the coupling terms in the two-phase fluid flow process and deformation process are handled by a mixture approach of monolithic and staggered schemes, i.e. equations of two-phase fluid flow process are solved in monolithic manner, while its coupling to deformation process is performed by staggered iterations, see Sanavia et al. [48]. Moreover a pressure–pressure scheme is applied to the two-phase flow model for convenience in stress calculation in porous media. With the present assumption, the changes in flow and deformation fields of the model are simulated by using the standard Galerkin finite element method, which is realized in the object-oriented scientific tool OpenGeoSys (OGS) [31]. OGS is an open source scientific software platform for numerical analysis for applications in hydrology [5], geotechnics [30], waste management [3], geothermics [29] and provides a large variety of interfaces for code coupling to other environmental disciplines such as soil science and climate research [27]. In this paper we focus on the framework for numerical modeling of non-isothermal two-phase consolidation processes related to Carbon Capture and Sequestration (CCS) technology. Concerning the practical and environmental relevance of the CCS we refer to Görke et al. [22]. As an extension to prior work, in this study we adopt the numerical framework to CO₂ storage problems which requires an extension of governing balance equations as well as the corresponding equations of state for CO₂. During CCS operations, carbon dioxide can occur at different thermodynamic states, liquid, gaseous or supercritical ones.

2. Model formulation

From the mechanical point of view we consider non-isothermal flow of two fluid phases (compressible and incompressible fluids) in a deformable thermo-poro-elastic porous medium based on Biot's consolidation concept – a thermo-hydro-mechanical (TH²M) coupled field problem, see de Boer [16] and Faust and Mercer [19].

Fig. 1 shows the conceptual model of a porous medium consisting of several fluid and solid phases. Different fluids (air, CO, water, and non-aqueous phase liquids (NAPL)) can coexist within the pore space. The interaction of fluids

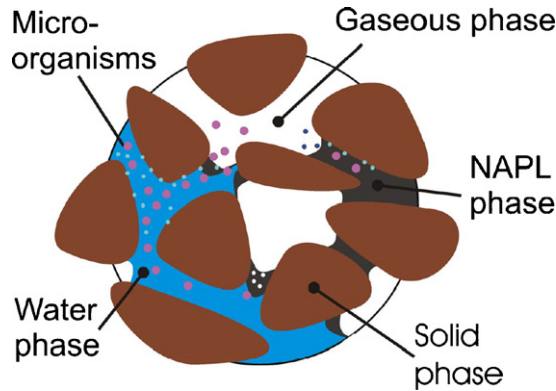


Fig. 1. Concept of porous media mechanics.

and the solid skeleton of the porous medium are denoted as consolidation [22]. Chemical species can be dissolved in pore fluids or adsorbed onto solid grain surfaces. In case of non-isothermal processes the thermal energy balance needs to be taken into account [58]. The concept of volume fraction is used to describe the portion of individual phases in the porous medium, i.e. by volume fractions $\epsilon_i = V_i/V$. All quantities are described in a list of symbols (Table 2).

Similar multi-field problems need to be solved for geotechnical applications such as subsurface waste deposition, see Rutqvist et al. [47], Kalbacher et al. [28], Singh et al. [49], and Blaheta and Nedoma [11].

The followings steps have to be conducted to derive the general field equations in terms of primary field variables, see Hassanizadeh and Gray [24]:

- (1) Macroscopic balance equations for mass, momentum and energy conservation of the multi-phase porous medium.
- (2) Constitutive relationships for non-isothermal multiphase processes in deformable porous media, see Benes and Mayer [6].
- (3) Applying the constitutive relationships and introducing physically based simplifications to the balance equations for the derivation of the general field equations.

In this work we present a general and concise formulation of TH²M problems. This should enable us to use the theoretical THM framework also for applications beyond CCS, such as geothermal reservoirs and nuclear waste depositories. The differences “simply” are the material properties of the geomaterials as well as the $p - T$ conditions.

2.1. Balance equations

In the following subsections we present the theoretical framework for THM modeling in a concise way. References are given to related works going into more details, e.g. Lewis and Schrefler [36], Baggio et al. [2], and Kolditz et al. [33]. Normally flow and subsequent transport processes in porous media for groundwater applications are associated with non-deformable, static media. In this case the seepage velocity is defined by Darcys law. If deformation processes of the solid phase of the porous medium are important to be included as for many geotechnical applications such as carbon dioxide sequestration, geothermal energy, nuclear waste deposition, the balance equations have to be modified

Table 1
Possible selections of primary variables for TH²M problems.

Process	H	H	T	M
pp formulation	$p^1 == p_c$	$p^2 == p^g$	T	\mathbf{u}
pS formulation	p^1	S^2	T	\mathbf{u}

correspondingly. In case of deformable porous media a γ fluid phase Darcy velocity $\mathbf{v}^{\gamma s}$ relative to the solid phase s is being used, see Eq. (4). We briefly recall the macroscopic porous medium balance equations for:

- Mass conservation

$$n \sum_{\gamma} S^{\gamma} \dot{\rho}^{\gamma} + n \sum_{\gamma} \rho^{\gamma} \dot{S}^{\gamma} + \sum_{\gamma} (n S^{\gamma} \rho^{\gamma} \mathbf{v}^{\gamma s}) + \left(\sum_{\gamma} S^{\gamma} \rho^{\gamma} \right) (\rho^s \nabla \cdot \mathbf{v}^s + (1 - n) \dot{\rho}^s) = \sum_i Q^i \quad (1)$$

Note that summation index γ is for fluid phases only, index i is sums both fluid and solid phases.

- Momentum conservation

$$\nabla \cdot (\boldsymbol{\sigma} - \alpha_b \left(\sum_{\gamma} S^{\gamma} p^{\gamma} \right) \mathbf{I} - \beta_T T (3\lambda + 2G) \mathbf{I}) = \rho \mathbf{g} \quad (2)$$

where λ is the Lamé constant, G is the shear modulus, and α_b is Biot's coefficient.

- Energy conservation

$$c \rho \dot{T} + \underbrace{\nabla \cdot \left(\sum_{\gamma} \rho^{\gamma} \mathbf{v}^{\gamma} c^{\gamma} T \right)}_{\text{advective part}} - \underbrace{\sum_i \lambda_{Ti} \nabla T}_{\text{conductive part}} = \rho Q_h + \mathbf{v} \cdot \nabla \sigma \quad (3)$$

Remarks:

- Mass conservation: in contrast to classic consolidation theory we cannot assume grain incompressibility (i.e. $\dot{\rho}^s = 0$) if thermo-elastic phenomena become important.
- Momentum conservation:
 - Inertial forces can be neglected for porous media flow.
 - Fluid momentum balance is represented by Darcy's law as a constitutive flux expression.
- Energy conservation:
 - The procedure in order to derive a heat balance equation from energy conservation is shown in Kolditz and Diersch [32].
 - Latent heat effects are included into heat capacity calculation.
- Symbols: no phase specification (exponent) means property of the porous medium, i.e. $\beta_T = \sum_i \epsilon^i \beta_T^i$. Fluid phases are denoted by γ .

2.2. Constitutive equations

The above balance equations are formulated independent from specific materials constraints, i.e. the formulations are very general and, therefore, applicable to a large variety of TH²M problems. The balance equations have to be closed by thermodynamic fluxes (Section 2.2.1) and equations of state (Section 2.2.2), see Gawin et al. [21]. The constitutive theory of porous media is discussed in great detail including historical aspects in [15]. Concerning concepts and implementation of constitutive relationships of porous media solid mechanics within the OGS numerical framework we refer to Görke et al. [22] and Watanabe et al. [60] for geotechnical and geothermal field applications.

2.2.1. Fluxes

- Fluid flux – Darcy's law

The relationship for fluid fluxes in porous media, i.e. Darcy's law, can be considered as a phenomenological equation. This means the fluid flux is assumed to be proportional to the pressure gradient and the gravity force.

$$\mathbf{J}_H^{\gamma s} = n S^{\gamma} \underbrace{(\mathbf{v}^{\gamma} - \mathbf{v}^s)}_{\mathbf{v}^{\gamma s}} = -n S^{\gamma} \left(\frac{k_{\text{rel}}^{\gamma} \mathbf{k}}{\mu^{\gamma}} (\nabla p^{\gamma} - \rho^{\gamma} \mathbf{g}) \right) \quad (4)$$

- Heat flux – Fourier's law

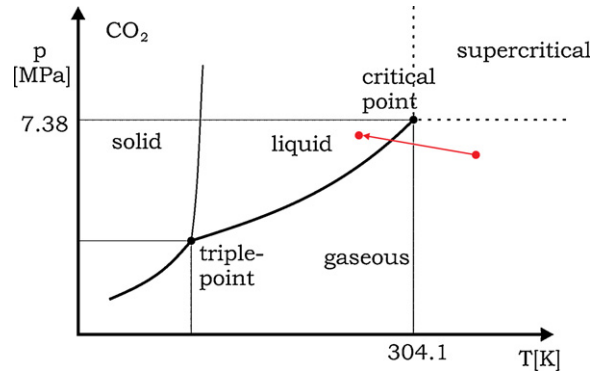


Fig. 2. Phase diagram of carbon dioxide. (For interpretation of the references to color in the text, the reader is referred to the web version of the article.)

Total diffusive heat flux in the isotropic porous medium is given by Fourier’s law for heat conduction

$$\mathbf{J}_T = -\lambda \nabla T \tag{5}$$

- Vapour flux

In multi-phase systems containing gases the transport of water vapor (i.e. water species in the gaseous phase) driven by pressure and temperature gradients needs to be taken into account, see Olivella and Gens [41].

$$\mathbf{q}_w^g = -D_{pv} \nabla p^g - f_{Tv} D_{Tv} \nabla T \tag{6}$$

where f_{Tv} is a thermal diffusion enhancement factor with a value of 1.0 in the present work, D_{pv} and D_{Tv} are diffusion coefficients takes the form as

$$D_{pv} = \frac{D_v \rho_v}{\rho_w R T_{abs}}$$

$$D_{Tv} = D_v \left(h \frac{\partial \rho_v S}{\partial T} - \frac{\rho_v P}{\rho_w R T_{abs}^2} \right) \tag{7}$$

2.2.2. Equations of state

For the TH²M problem under consideration we have to include appropriate equations of state (EOS) for the following material properties:

- Density
- Viscosity
- Capillary pressure
- Relative permeability
- Heat capacity
- Heat conductivity
- Stress–strain relationships (plasticity and creep)

The constitutive relations are depending on state variables. As the thermodynamical state variables change significantly during CO₂ injection into the subsurface, phase changes of the involved fluids may become important. Fig. 2 depicts the phase diagram of carbon dioxide. The red line in Fig. 2 shows a path in the phase diagram if CO₂ is cooled from 400 K to 300 K and pressurized from 6.5 MPa up to 7 MPa. Under these circumstances carbon dioxide will change from hot gas to a liquid state.

A very rigorous thermodynamic approach to the description of variable fluid properties is the use of the free Helmholtz energy,

$$\frac{f(p, T)}{RT} = \phi(\delta, \tau) = \phi^o(\delta, \tau) + \phi^r(\delta, \tau) \tag{8}$$

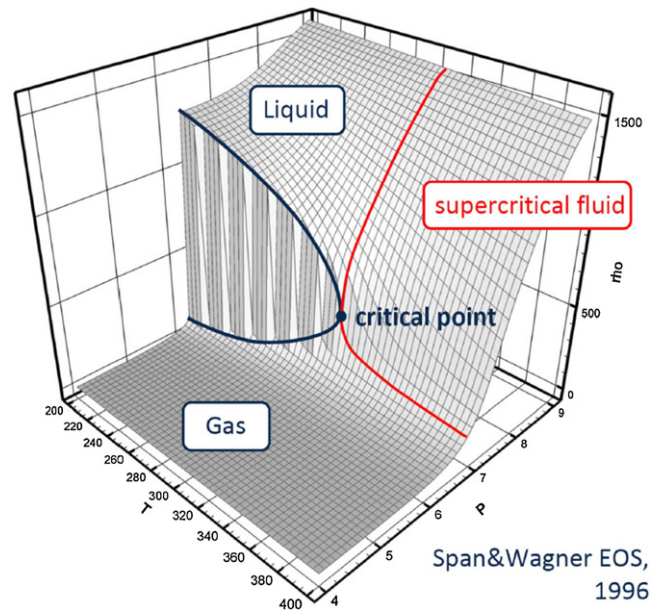


Fig. 3. CO₂ density as a function of pressure and temperature.

where $\delta = \rho/\rho_c$ and $\tau = T_c/T$ are dimensionless quantities, ρ_c and T_c represents the values at the critical point (see [17,18]). Based on the free Helmholtz energy, equations of state for any fluids can be derived. As an example the density function of CO₂ is depicted in Fig. 3, see Span and Wagner [53].

2.3. General balance equations

The mathematical formulations of THM and TH² problems for single-phase non-isothermal consolidation and non-isothermal two-phase flow are in detail described in Wang et al. [58], respectively. The idea of this section is to develop a generic mathematical description for combined TH²M problem classes which are suited for object-oriented implementation. The related primary variables of TH²M problems are two fluid phase pressures p^1, p^2 , the displacement vector \mathbf{u} and temperature T , respectively. The meaning of fluid pressure can be different for specific H² problems, i.e. fluid phase or capillary pressure (Table 1). Finally, the governing equations are written in terms of primary variables for the TH²M problem. Depending on the two different formulations for the two-phase flow problem, the primary variables for the second fluid phase are pressure or saturation, respectively (Table 1). The selection of appropriate primary variables is essential for the numerical solution of coupled multi-field problems. Park et al. [42] discussed the numerical accuracy by solving two-phase flow problems related to CCS in saline aquifers. Proper selection of primary variables can even avoid inaccurate numerical schemes such as upwinding techniques. In order to develop a universal description of the mathematical formulation for TH²M problems with varying primary variables, we introduce the following notation:

- p^1, p^2, T, \mathbf{u} : primary variables,
- H, T, M : coefficient matrices for hydraulic, thermal, mechanical processes, respectively,
- Q : right-hand-side terms representing source/sink terms,
- Indices t, xx, tx : related to temporal (t) and spatial (x) derivatives, respectively,
- Indices H, T, M : related to hydraulic (H), thermal (T), mechanical (M) processes, respectively.

This generic mathematical framework has proved very useful for the object-oriented code implementation of TH²M problems.

Table 2
List of symbols.

Symbol	Definition	Unit
c	Specific heat capacity	J/kg K
D_{pv}, D_{Tv}	Vapor diffusion coefficients	m ² /Pa s, m ² /K s
f	Free Helmholtz energy	J
G	Shear modulus	Pa
\mathbf{g}	Gravity vector	m/s ²
\mathbf{J}	Flux vector	–
\mathbf{k}	Permeability tensor	m ²
k_{rel}	Relative permeability function	–
n	Porosity	–
p	Pressure	Pa
\mathbf{q}	Darcy velocity vector	m/s
Q	Source/sink term	–
R	Ideal gas constant	J/mol K
S	Saturation	–
T	Temperature	K
\mathbf{u}	Displacement vector	m
\mathbf{v}	Velocity	m/s
α_b	Biot coefficient	–
β_T	Thermal expansion coefficient	1/K
ϵ	Volume fraction	–
λ_T	Thermal conductivity	W/mK
λ	Lame coefficient	Pa
μ	Viscosity	Pa s
ρ	Density	kg/m ³
σ	Stress tensor	Pa
A^γ	Fluid quantity	–
A^s	Solid quantity	–
A^T	Transpose quantity	–
$A^{\gamma s}$	Quantity of phase γ relative to phase s , e.g., seepage velocity	–
A_v	Vapor quantity	–
A_H	Hydraulic quantity	–
A_T	Thermal quantity	–
A_M	Mechanical quantity	–
H_t, H_{xx}	Coupling matrices for hydraulic processes (time, space)	–
M_t, H_{xx}	Coupling matrices for mechanical processes (time, space)	–
T_t, H_{xx}	Coupling matrices for thermal processes (time, space)	–
$\dot{}$	Time derivative	–
∇A	Space derivative, gradient	–
$\nabla \cdot \mathbf{A}$	Space derivative, divergence	–

2.3.1. Non-isothermal two-phase flow in a deformable porous medium

The general flow equation of the TH²M problem is:

$$\begin{aligned}
 & H_t^1 \dot{p}^1 + H_{xx}^1 \nabla^T \cdot \nabla p^1 + \\
 & \quad + H_{xx}^2 \nabla^T \cdot \nabla p^2 + \\
 & HT_t \dot{T} + \\
 & HM_{tx} \nabla \dot{\mathbf{u}} + \\
 & \quad = Q_H + Q_{HT}
 \end{aligned} \tag{9}$$

with the following equation coefficients:

$$\begin{aligned}
 H_t^1 &= n \left((\rho^l - \rho_w^g) \frac{\partial S^l}{\partial p_c} + (1 - S^l) \frac{\partial \rho_w^g}{\partial p_c} \right) \\
 H_{xx}^1 &= \rho^l \frac{\mathbf{k}k_{\text{rel}}^l}{\mu^l} \\
 H_{xx}^2 &= \rho_w^g \frac{\mathbf{k}k_{\text{rel}}^g}{\mu^g} - \rho^l \frac{\mathbf{k}k_{\text{rel}}^l}{\mu^l} \\
 HT_t &= n \left((\rho^l - \rho_w^g) \frac{\partial S^l}{\partial T} + (1 - S^l) \frac{\partial \rho_w^g}{\partial T} \right) - \beta_T \\
 HM_{tx} &= S^l \rho^l + (1 - S^l) \rho_w^l \\
 Q_H &= - \left(\rho^l \frac{\mathbf{k}k_{\text{rel}}^l}{\mu^l} \rho^l + \rho_w^g \frac{\mathbf{k}k_{\text{rel}}^g}{\mu^g} \rho^g \right) \mathbf{g} \\
 Q_{HT} &= \nabla \left(\rho^g \frac{M_a M_w}{M_g^2} D_w^g \nabla \left(\frac{p_w^g}{p^g} \right) \right)
 \end{aligned} \tag{10}$$

2.3.2. Two-phase flow heat transport in a deformable porous medium

The general heat transport equation of the TH²M problem is:

$$T_t \dot{T} + T_x \nabla T + T_{xx} \nabla^T \cdot \nabla T = Q_T + Q_{TM} \tag{11}$$

with the following equation coefficients:

$$\begin{aligned}
 T_t &= \sum_i \epsilon^i c^i \rho^i \\
 T_x &= n \sum_\gamma S^\gamma c^\gamma \rho^\gamma \mathbf{v}^{\gamma s} \\
 T_{xx} &= \sum_i \epsilon^i \lambda_{Ti} \\
 Q_T &= \rho q_T \\
 Q_{TM} &= \mathbf{v} \cdot \nabla \boldsymbol{\sigma}
 \end{aligned} \tag{12}$$

2.3.3. Non-isothermal two-phase flow consolidation

The general equation for stress equilibrium of the TH²M problem is:

$$\begin{aligned}
 &MH_x^1 \nabla p^1 + \\
 &MH_x^2 \nabla p^2 + \\
 &MT_x \nabla T + \\
 &M_{xx} \nabla^T \cdot \nabla \mathbf{u} + \\
 &= Q_M + Q_{MH} + Q_{MT}
 \end{aligned} \tag{13}$$

with the following equation coefficients:

$$\begin{aligned}
 MH_x^1 &= \alpha_b S^1 \\
 MH_x^2 &= \alpha_b S^2 \\
 MT_x &= \beta_T = \sum_i \epsilon^i \beta_T^i \\
 M_{xx} &= \mathbf{C} \\
 Q_M &= \rho \mathbf{g} = \left(\sum_i \epsilon^i \rho^i \right) \mathbf{g}
 \end{aligned}
 \tag{14}$$

3. Computational scheme

3.1. Numerical method

The method of weighted residuals is applied to derive the weak formulations of all the governing equations given above (Section 2), which results in a system of nonlinear algebraic equations. For the time discretization we use the generalized first order difference scheme. The nonlinear coupled boundary value problem is solved iteratively using the Picard linearization within the context of the finite element method, see Lewis and Schrefler [36]. A corresponding mixed finite element scheme is presented by Truty and Zimmermann [54]. Alternatively, higher-order Newton schemes can be deployed for solving non-linear problems. However those schemes require a sufficient accurate initial guess which might be difficult to obtain for TH²M problems. Therefore a tradeoff between accuracy and robustness has to be considered. We use different types of finite elements in order to guarantee the same numerical accuracy of different PDE types, i.e. linear elements are used for flow and heat transport, quadratic elements are applied to the deformation process.

$$\underbrace{\begin{bmatrix} C_{uu} & C_{u1} & C_{u2} & C_{ut} \\ C_{1u} & C_{11} & C_{12} & C_{1t} \\ C_{2u} & C_{21} & C_{22} & C_{2t} \\ 0 & C_{t1} & C_{t2} & C_{tt} \end{bmatrix}}_{\mathbf{C}} \frac{d}{dt} \underbrace{\begin{Bmatrix} \hat{\mathbf{u}} \\ \hat{\mathbf{p}}^1 \\ \hat{\mathbf{p}}^2 \\ \hat{\mathbf{T}} \end{Bmatrix}}_{\mathbf{x}} + \underbrace{\begin{bmatrix} K_{uu} & K_{u1} & K_{u2} & K_{ut} \\ 0 & K_{11} & K_{12} & 0 \\ 0 & K_{21} & K_{22} & 0 \\ 0 & K_{t1} & K_{t2} & K_{tt} \end{bmatrix}}_{\mathbf{K}} \underbrace{\begin{Bmatrix} \hat{\mathbf{u}} \\ \hat{\mathbf{p}}^1 \\ \hat{\mathbf{p}}^2 \\ \hat{\mathbf{T}} \end{Bmatrix}}_{\mathbf{x}} = \underbrace{\begin{Bmatrix} \mathbf{r}^u \\ \mathbf{r}^1 \\ \mathbf{r}^2 \\ \mathbf{r}^t \end{Bmatrix}}_{\mathbf{r}}
 \tag{15}$$

Still more compact, we can write,

$$\mathbf{C}(\mathbf{x}) \frac{d}{dt} \mathbf{x} + \mathbf{K}(\mathbf{x}) \mathbf{x} = \mathbf{r}(\mathbf{x})
 \tag{16}$$

3.2. Coupling scheme

For two-phase flow equations, the choice of primary variables is of crucial importance for the stability of the employed numerical scheme. Since we simulate hydraulic mechanical coupled problems, we select capillary pressure and CO₂ pressure as primary variables. After discretizing the above weak forms for the TH²M problem, we obtain a system of algebraic equations written in compact matrix notation. A parallel scheme for finite element analysis of THM coupled processes is presented e.g. by Wang et al. [59], Blaheta et al. [10].

An adaptive time stepping scheme is used for temporal discretization of the coupled multi-field problem [59]. We employ the PI (proportional and integral feedback) [23] classic time control method, which provides a stable and efficient time stepping for the numerical solution of PDEs. The idea behind PI control is the elementary local error control theory, i.e. the next time step size, Δt^{n+1} can be predicted by the local error estimation [52].

Two methods for solving non-linear problems are available in OGS, Newton and Picard iterations. We use the Newton method for non-coupled non-linear problems such as inelastic deformation processes. For coupled non-linear

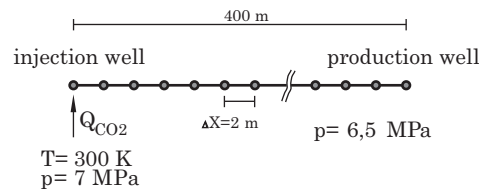


Fig. 4. Model set-up.

problems we apply fixpoint iteration schemes (Picard method) due to more robustness but less convergence speed [32]. The BICGStab iterative method is used for solving the linearized algebraic equation systems.

4. Examples

Numerical simulation of coupled TH²M processes including possible phase changes is a complex task. In order to verify the computational schemes a systematic collection of benchmarks needs to be developed [30]. Here we present results for three new test cases: (1) a 1-D case to investigate the influence of variable fluid properties, (2) a 2-D vertical cross-section to study the interaction between hydraulic and mechanical forces, and (3) a 3-D case to test the stability and computational costs of the two-phase flow models for real applications. Additional verification example for TH²M sub-processes can be found e.g. in Korsawe et al. [34], McWorther and Sunada [38] and Nordbotten and Celia [40]. Recently, in the scope of the CLEAN project CO₂ storage in depleted gas reservoirs has been investigated in detail related to the development of monitoring concepts and conceptual modeling approaches [25,12,51,50]. The MoPa project was dealing with the investigation of deep saline aquifers for CO₂ storage concerning both monitoring and modeling [4,7,43,35].

4.1. 1-D case: variable fluid properties

We consider non-isothermal compressible CO₂ flow between two boreholes taking into account pressure and temperature dependent density and viscosity. The initial pressure of the reservoir is set to 6.5 MPa, the pressure in the injection well amounts to 7.0 MPa. At the beginning of the infiltration, the reservoir has a temperature of 400 K, so the reservoir is filled with gas. The injected CO₂ is liquid; it has a temperature of 300 K. During the infiltration process, the reservoir will cool down and the fluid will change its phase (see Fig. 2). This model setup consists of 200 line elements with a length of 2 m. There is an injection well on the left, and a production well on the right side (see Fig. 4).

Fig. 5 shows the distribution of the fluid density and its viscosity after a simulation time of 50,000 s. At this time, the phase border has moved 175 m away from the injection well. At this point, the density jumps from 475 kg/m³ to 220 kg/m³. The stepwise dropping of density between 175 m and 300 m is caused by the interpolation of database values. A higher resolution of density values in the database should solve this problem. The “saw teeth” and the offset between 60 m and 120 m is also caused by the interpolation, but this time the problem is deeper. Here, the interpolation takes place between liquid and gaseous density values. To solve this problem, the EOS-reading function has to be enhanced by a switch which avoids an interphase interpolation.

4.2. 2-D case: two-phase flow consolidation

The second example represents CO₂ injection using an axisymmetric TH²M model (flow of water and liquid CO₂). The deep saline aquifer is located at a depth of 770 m below the ground surface and has a thickness of 6 m, as illustrated in Fig. 6. The saline aquifer is fully saturated with water before injection.

In the present study, the near field is the domain of interest. To this purpose, we assume the problem is axisymmetrical in both geometry and physics. The axi-symmetric model domain is bounded on the inner side by the wellbore radius of 0.2 m. The outer boundary is at a radius of 200 m. In the simulation, the density of the two liquid phases and the solid phase are assumed to be constant. The Brook–Corey model is employed to parameterize the hydraulic properties of liquid CO₂ and water.

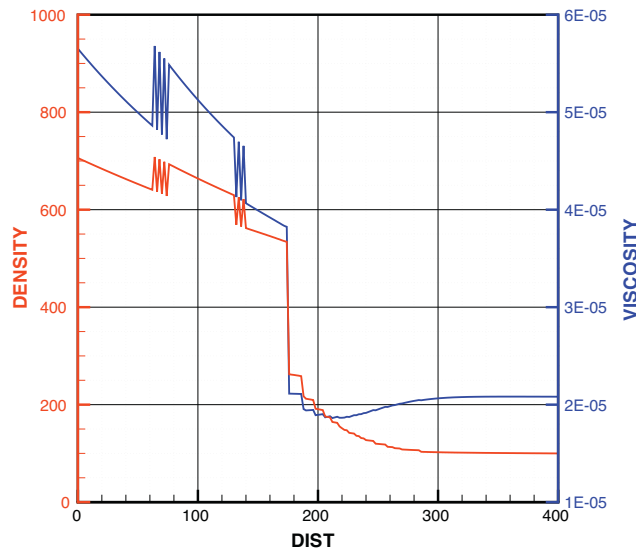


Fig. 5. Density [kg/m³] and viscosity [Pa s] of CO₂ calculated during the simulation.

The problem is solved in two stages. Initially, the stresses in the deep saline aquifer are assumed to be produced by the gravity force only, and the distribution of them is calculated by solving the stress equilibrium equation with the volume force term. Later on, the stress results obtained by the initial distribution analysis are used as the initial stress status for CO₂ injection modeling in the second phase.

A constant Neumann condition of 0.4475×10^{-5} m/s is applied at the injection well wall for hydraulic equation to represent the injection rate of CO₂. Maximum water saturation and residual CO₂ saturation are assigned in the Dirichlet outer boundary conditions. On top and bottom surfaces, the displacement in vertical direction is fixed. Top and bottom surfaces are impervious (no flow boundaries).

In order to investigate the impact of solid deformation on the hydraulic field, we conduct simulations of the two-phase flow process in the deep saline aquifer by taking account of and neglecting the deformation coupling. To demonstrate this impact, we plot in Fig. 7 the CO₂ saturation for a period of 1000 h at two specified observation points, which are 20 m and 50 m far away from injection well, respectively.

Fig. 7 portrays that the propagation of CO₂ is enhanced by deformation because saturations rise faster and to higher values compared to the static case without deformation processes. On the other hand, the stress field is significantly altered by the CO₂ injection pressure. We can clearly see stress change at the two observation points as depicted in Fig. 8. The tangent stress decreases at the beginning of the injection due to the extension at the well surface, and then increases due to propagation of the injection pressure. Since we assume the initial stress is only induced by the gravity

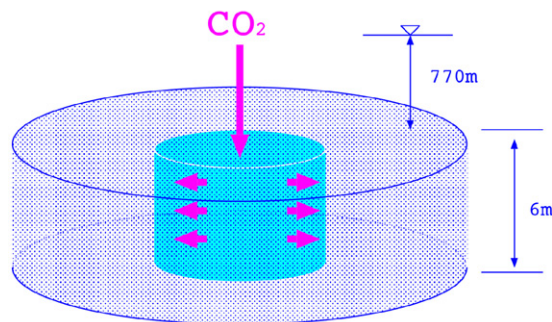


Fig. 6. CO₂ injection model.

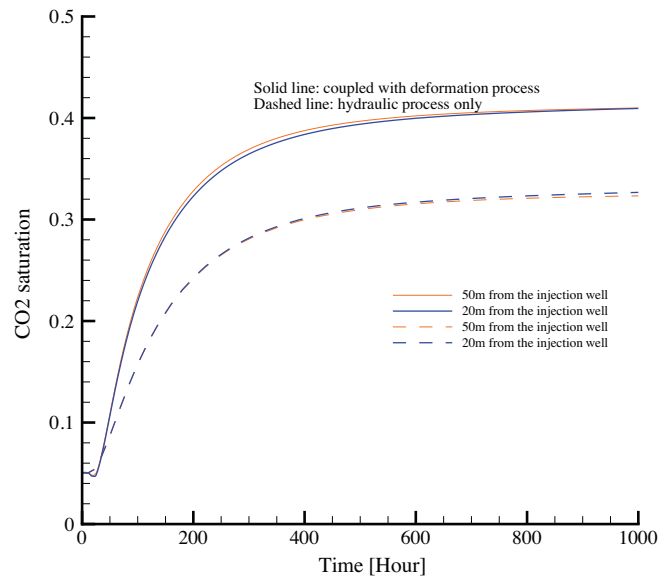


Fig. 7. Evolution of CO₂ saturation at two observation points.

force, the initial stress distribution in the analyzed domain is a vertical gradient. Due to the injection pressure of CO₂, the stress in the tangent direction increases significantly.

Fig. 9 shows the distribution of tangent stress and CO₂ saturations near the injection well at the time of 1 h and 1000 h. Comparing both figures, we see that the distribution patterns of tangent stress and CO₂ saturations are quite similar, which explains the coupling between hydraulic and mechanical processes.

4.3. 3-D case: approaching reality

The last example is based on benchmark definitions for approaching reality [13]. The test case is a H^2M 3-D model of two aquifers which are penetrated by two boreholes. We use about 100,000 finite elements for spatial discretization

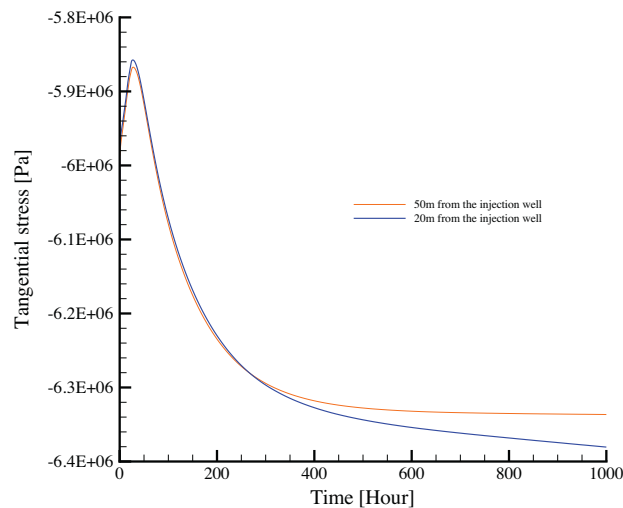


Fig. 8. Evolution of tangent stress at two observation points.

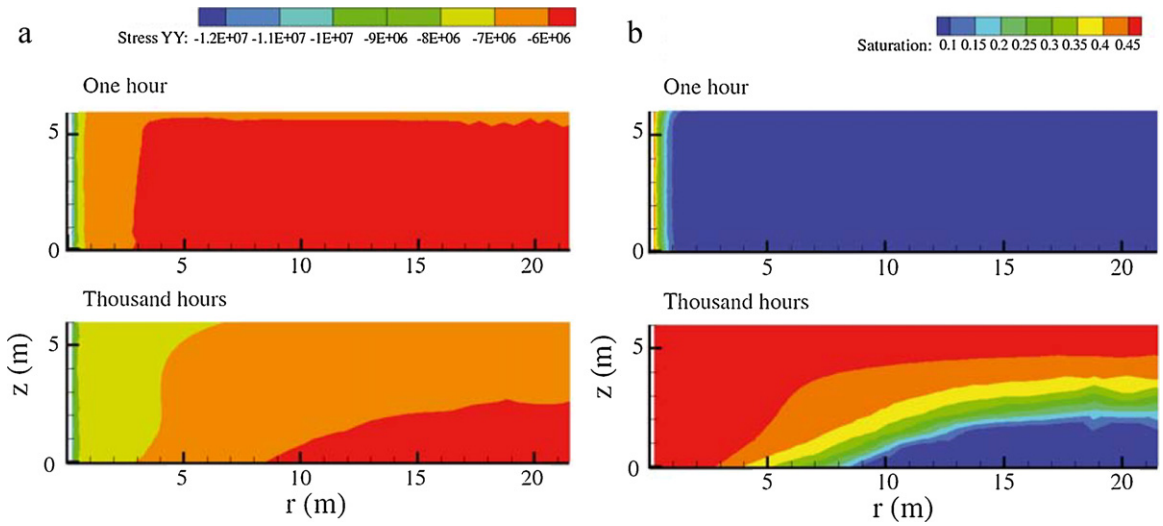


Fig. 9. Distribution of tangent stress (left) and CO₂ saturation (right) at the beginning of injection and after 1000 h injection.

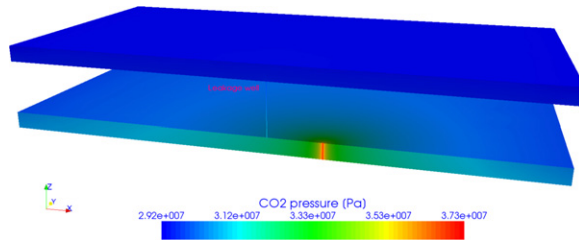


Fig. 10. Results of the 3-D two-phase flow simulation: liquid phase pressure of CO₂.

(linear elements for pressure and quadratic elements for deformation). CO₂ is injected into the lower aquifer. The purpose of the modeling study is to analyse the CO₂ leakage to the upper aquifer through a borehole 400 m from the injection well. Figs. 10 and 11 show the results of the 3-D two-phase (H²) simulations. Liquid pressure and saturation of CO₂ is plotted for a selected time. The plots show the radial propagation of carbon dioxide. We see the density effect of upconing CO₂ due to the smaller density in comparison to the saline water. The carbon dioxide reaches the leaky well after about 100 days.

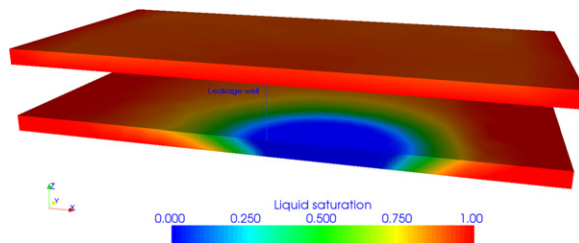


Fig. 11. Results of the 3-D two-phase flow simulation: liquid (water) saturation.

5. Conclusions

This paper reports ongoing work on developing the theoretical and numerical framework as well as object-oriented software for the solution of thermo-hydro-mechanical–chemical (THMC) coupled problems related to CO₂ storage in the geologic subsurface. Additional phenomena of interest for carbon dioxide sequestration are chemical processes, see Pont and Ehrlicher [44], convection processes, see Riaz et al. [46] and fracturing, see Walsh et al. [56].

In this paper we developed a conceptual approach for non-isothermal multi-phase flow consolidation in porous media. The corresponding TH²M model is numerically solved using the finite element method. Three test examples are presented in order to discuss details of TH²M processes, such as variable fluid properties exhibiting phase changes, interaction of capillarity and buoyancy forces, and two-phase flow in 3-D aquifer structures. The current status of the presented TH²M method is not solving the problem but rather pointing to important details of the coupled system.

In the numerical analysis of CO₂ storage, most of the work reported in literature focuses on the hydraulic or chemical changes during injection or storage. With a simple axisymmetrical example of two-phase flow and deformation coupled processes in the saline aquifers, we demonstrate that the stress change in the vicinity of the CO₂ injection well is distinct from the initial stress state, and such coupling must be considered as an issue for the assessment of the safety of injection and storage. The newly developed numerical scheme for pressure–pressure based two-phase flow provides stable and accurate results.

The present TH²M concept is more general in comparison to Wang and Kolditz [57], as in addition to CO₂ sequestration it can be extended to geothermal reservoir analysis and safety assessment of nuclear waste repositories. To this purpose the properties of the corresponding geofluids and geological environment, i.e. equations of state and constitutive equations, need to be specified accordingly.

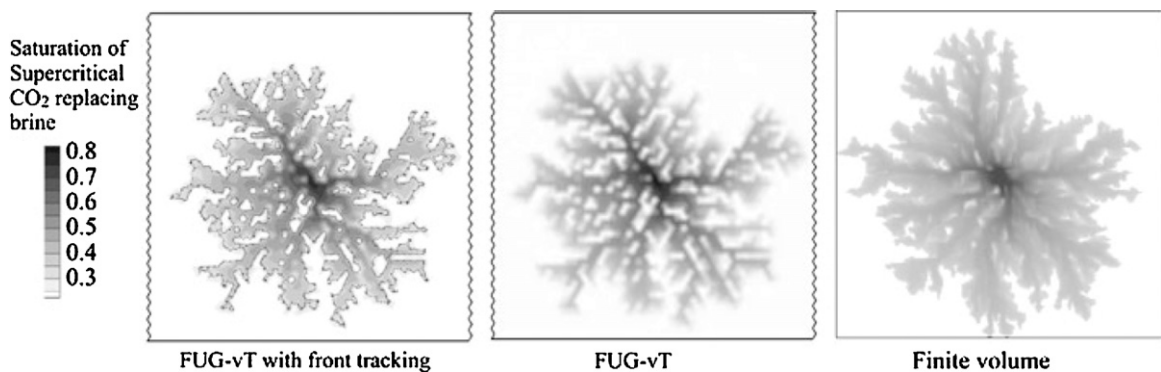


Fig. 12. Influence of reservoir heterogeneity to CO₂ distribution.

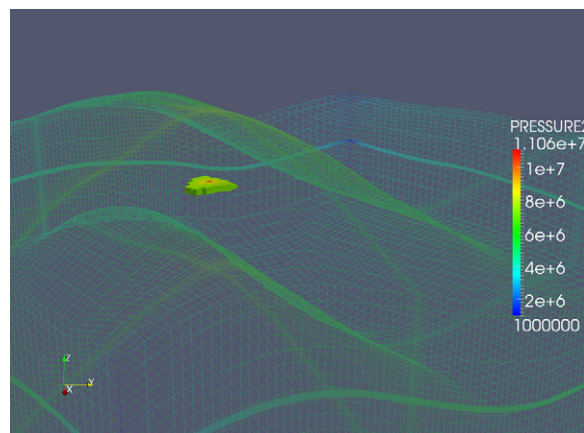


Fig. 13. Simulation of CO₂ distribution in an off-shore site in the North Sea.

Concerning future research in CO₂ modeling, very important is to address issues related to heterogeneity and reality (i.e. data availability from field tests). Fig. 12 illustrates the impact of heterogeneity in subsurface reservoirs McDermott et al. [37]. In this figure the front tracking location is presented, then removed for comparison to the finite volume (FV) approach. The FV calculation was implemented in the Quintessa Ltd. Multi-Physics code QPAC (www.quintessa.org/qpac), adopting the same element structure for the finite volume grid. The reliability of CO₂ modeling will depend to a large extent on data availability. Several data sets are available now for model calibration purposes. Fig. 13 depicts the simulation of CO₂ pressure distribution using data from a real reservoir in the North Sea.

Acknowledgements

The funding by the German Federal Ministry of Education and Research (BMBF) under grants 03G0760F (CO2MAN), 03G0797D (CO2BENCH), 03G0686D (CO2-MoPa) and 03E10588 (A-DuR) is greatly acknowledged. We would like to thank Prof. Blaheta to provide us the opportunity to present this paper on the Modeling 2009 conference in Roznov, Czechia. The material of this paper has been presented at this conference.

References

- [1] R. Arts, O. Eiken, A. Chadwick, P. Zweigel, L. van der Meer, B. Zinszner, Monitoring of CO₂ injected at Sleipner using time-lapse seismic data, *Energy* 29 (2004) 1383–1392.
- [2] P. Baggio, C. Bonachina, B.A. Schrefler, Some considerations on modeling heat and mass transfer in porous media, *Transport in Porous Media* 28 (2004) 233–251.
- [3] S. Bauer, C. Beyer, O. Kolditz, Assessing measurement uncertainty of first-order degradation rates in heterogeneous aquifers, *Water Resources Research* 42 (2006) W01420, <http://dx.doi.org/10.1029/2004WR003878>.
- [4] S. Bauer, H. Class, M. Ebert, V. Feeser, H. Goetze, A. Holzheid, O. Kolditz, S. Rosenbaum, W. Rabbel, D. Schaefer, A. Dahmke, Modeling and parameterization of CO₂ storage in deep saline formations for dimension and risk analyses – the CO₂-MoPa project, *Environmental Earth Sciences* 67 (2012), <http://dx.doi.org/10.1007/s12665-012-1707-y>.
- [5] M. Beinhorn, P. Dietrich, O. Kolditz, 3-d numerical evaluation of density effects on tracer tests, *Journal of Contaminant Hydrology* 81 (2005) 89–105.
- [6] M. Benes, P. Mayer, Coupled model of hygro-thermal behaviour of concrete during fire, *Journal of Computational and Applied Mathematics* 281 (2008) 12–20.
- [7] C. Beyer, D. Li, M. de Lucia, M. Kuehn, S. Bauer, Modelling CO₂-induced fluid–rock interactions in the Altensalzwedel gas reservoir. Part II – Coupled reactive transport simulations, *Environmental Earth Sciences* 67 (2012), <http://dx.doi.org/10.1007/s12665-012-1684-1>.
- [8] A. Bielinski, Numerical simulation of CO₂ sequestration in geological formations, Ph.D. thesis, Institute of Hydraulic Engineering, University of Stuttgart, 2007.
- [9] J. Birkholzer, Q. Zhou, C.-F. Tsang, Large-scale impact of CO₂ storage in deep saline aquifers: a sensitivity study on pressure response in stratified systems, *International Journal of Greenhouse Gas Control* 3 (2008) 181–194.
- [10] R. Blaheta, P. Byczanski, O. Jakl, R. Kohut, A. Kolcun, K. Krecmer, J. Stary, Large scale parallel fem computations of far/near stress field changes in rocks, *Future Generation Computer Systems – The International Journal of Grid Computing Theory Methods and Applications* 22 (2006) 449–459.
- [11] R. Blaheta, J. Nedoma, Special section: numerical modelling in geomechanics and geodynamics, *Future Generation Computer Systems – The International Journal of Grid Computing Theory Methods and Applications* 22 (2006) 447–448.
- [12] N. Böttcher, O. Kolditz, R. Liedl, Evaluation of equations of state for CO₂ in numerical simulations, *Environmental Earth Sciences* 67 (2012), <http://dx.doi.org/10.1007/s12665-012-1704-1>.
- [13] H. Class, A benchmark study on problems related to CO₂ storage in geologic formations, *Computational Geosciences* 13 (2009) 409–434.
- [14] D.B. Das, S.M. Hassanizadeh, *Upscaling Multiphase Flow in Porous Media – From Pore to Core and Beyond*, Springer, Dordrecht, 2005.
- [15] R. de Boer, *Theory of Porous Media: Highlights in Historical Development and Current State*, Springer, Berlin-Heidelberg, 2000.
- [16] R. de Boer, *Trends in Continuum Mechanics of Porous Media: Theory and Applications of Transport in Porous Media*, Springer, Heidelberg, 2005.
- [17] M. Dentz, D. Tartakovsky, Abrupt-interface solution for carbon dioxide injection into porous media, *Transport in Porous Media* 51 (2008) 1–13.
- [18] C. Doughty, K. Pruess, Modeling supercritical carbon dioxide injection in heterogeneous porous media, *Vadose Zone Journal* (2004) 837–847.
- [19] C.R. Faust, J.W. Mercer, Geothermal reservoir simulation: 1. Mathematical model for liquid and vapor dominated hydrothermal system, *Water Resources Research* 15 (1979) 23–30.
- [20] A. Förster, R. Giese, C. Juhlin, B. Norden, N. Springer, The geology of the CO2SINK site: from regional scale to laboratory scale, in: *Proceedings of the 9th International Conference on Greenhouse Gas Control Technologies (GHGT-9)*, Washington, DC, 2008.
- [21] D. Gawin, F. Pesavento, B.A. Schrefler, Simulation of damage–permeability coupling in hygro-thermo-mechanical analysis of concrete at high temperature, *Communications in Numerical Methods in Engineering* 18 (2002) 113–119.
- [22] U.-J. Goerke, C.-H. Park, W. Wang, A. Singh, O. Kolditz, Numerical simulation of multiphase hydromechanical processes induced by CO₂ injection in deep saline aquifers, *Oil & Gas Science and Technology – Revue d'IFP Energies Nouvelles* 66 (2011) 105–118.

- [23] K. Gustafsson, M. Lundh, G. Söderlind, A PI stepsize control for the numerical solution of ordinary differential equations, *BIT* 28 (1988) 270–287.
- [24] M. Hassanizadeh, W.G. Gray, General conservation equations for multiphase systems: 1. Averaging technique, *Advances in Water Resources* 2 (1979) 131–144.
- [25] Z. Hou, Y. Gou, J. Taron, U.-J. Görke, O. Kolditz, Thermo-hydro-mechanical modeling of carbon dioxide injection for enhanced gas-recovery (CO₂-EGR): a benchmarking study for code comparison, *Environmental Earth Sciences* 67 (2012), <http://dx.doi.org/10.1007/s12665-012-1703-2>.
- [26] F. Javadpour, CO₂ injection in geological formations: determining macroscale coefficients from pore scale processes, *Transport in Porous Media* 79 (2009) 87–105.
- [27] T. Kalbacher, J.-O. Delfs, H. Shao, W. Wang, M. M.W., L. Samaniego, C. Schneider, A. Musolff, F. Centler, F. Sun, A. Hildebrandt, R. Liedl, D. Borchardt, P. Krebs, O. Kolditz, The IWAS-ToolBox: software coupling for an integrated water resources management, *Environmental Earth Sciences* 65 (2012) 1367–1380.
- [28] T. Kalbacher, R. Mettler, C. McDermott, W. Wang, G. Kosakowski, T. Taniguchi, O. Kolditz, Geometric modeling and object-oriented software concepts applied to a heterogeneous fractured network from the Grimsel rock laboratory, *Computers & Geosciences* 11 (2007) 9–26.
- [29] O. Kolditz, Modelling flow and heat transfer in fractured rocks: conceptual model of a 3-d deterministic fracture network, *Geothermics* 24 (1995) 451–470.
- [30] O. Kolditz, S. Bauer, C. Beyer, N. Böttcher, P. Dietrich, U.-J. Görke, T. Kalbacher, C.-H. Park, U. Sauer, C. Schuetze, H. Shao, A. Singh, J. Taron, W. Wang, N. Watanabe, A systematic benchmarking approach for geologic CO₂ injection and storage, *Environmental Earth Sciences* 67 (2012), <http://dx.doi.org/10.1007/s12665-012-1656-5>.
- [31] O. Kolditz, S. Bauer, L. Bilke, N. Böttcher, J. Delfs, T. Fischer, U. Görke, T. Kalbacher, G. Kosakowski, C. McDermott, C. Park, F. Radu, K. Rink, H. Shao, H. Shao, F. Sun, Y. Sun, A. Singh, J. Taron, M. Walther, W. Wang, N. Watanabe, N. Wu, M. Xie, W. Xu, B. Zehner, OpenGeoSys: an open-source initiative for numerical simulation of thermo-hydro-mechanical/chemical (THM/C) processes in porous media, *Environmental Earth Sciences* 67 (2012), <http://dx.doi.org/10.1007/s12665-012-1546-x>.
- [32] O. Kolditz, H.-J. Diersch, Quasi steady-state strategy for numerical simulation of geothermal circulation processes in hot dry rock fracture, *International Journal of Non-linear Mechanics* 28 (1993) 467–481.
- [33] O. Kolditz, H. Shao, U. Görke, W. Wang, Thermo-hydro-mechanical/chemical processes in porous media: benchmarks and examples, in: *Lecture Notes in Computational Science and Engineering*, vol. 86, Springer, Heidelberg, 2012.
- [34] J. Korsawe, G. Starke, W. Wang, O. Kolditz, Finite element analysis of poro-elastic consolidation in porous media: standard and mixed approaches, *Computer Methods in Applied Mechanics and Engineering* 195 (2006) 1096–1115.
- [35] S. Lamert, H. Geistlinger, U. Werban, C. Schütze, A. Peter, G. Hornbruch, A. Schulz, M. Pohlert, S. Kalia, M. Beyer, J. Großmann, A. Dahmke, P. Dietrich, Feasibility of geoelectrical monitoring and multiphase modelling for process understanding of gaseous CO₂ injection into a shallow aquifer, *Environmental Earth Sciences* 67 (2012), <http://dx.doi.org/10.1007/s12665-012-1669-0>.
- [36] R.W. Lewis, B.A. Schrefler, *The Finite Element Method in the Static and Dynamic Deformation and Consolidation of Porous Media*, Wiley, 1998.
- [37] C. McDermott, A. Bond, W. Wang, O. Kolditz, Front tracking using a hybrid analytical finite element approach for two-phase flow applied to supercritical CO₂ replacing brine in a heterogeneous reservoir and cap rock, *Transport in Porous Media* 90 (2011) 545–573.
- [38] D.B. McWhorter, D.K. Sunada, Exact integral solutions for two-phase flow, *Water Resources Research* 26 (1990) 399–413.
- [39] B. Metz, O. Davidson, H. de Cominck, M. Loos, L. Meyer, IPCC special report on carbon dioxide capture and storage. Prepared by Working Group III of the Intergovernmental Panel on Climate Change, Cambridge University Press, Cambridge, United Kingdom and New York, NY, USA, 2005.
- [40] J. Nordbotten, M. Celia, Similarity solutions for fluid injection into confined aquifers, *Journal of Fluid Mechanics* 561 (2006) 307–327.
- [41] S. Olivella, A. Gens, Vapour transport in low permeability unsaturated soil with capillary effects, *Transport in Porous Media* 40 (2004) 219–241.
- [42] C.-H. Park, N. Boettcher, W. Wang, O. Kolditz, Are upwind techniques in multi-phase flow models necessary? *Journal of Computational Physics* 230 (2011) 8304–8312.
- [43] A. Peter, H. Lamert, M. Beyer, G. Hornbruch, B. Heinrich, A. Schulz, H. Geistlinger, P. Schreiber, P. Dietrich, U. Werban, C. Vogt, H. Richnow, J. Grossmann, A. Dahmke, Investigation of the geochemical impact of CO₂ on shallow groundwater: design and implementation of a CO₂ injection test in Northeast Germany, *Environmental Earth Sciences* 67 (2012), <http://dx.doi.org/10.1007/s12665-012-1700-5>.
- [44] S.D. Pont, A. Ehrlicher, Numerical and experimental analysis of chemical dehydration, heat and mass transfer in a concrete hollow cylinder submitted to high temperatures, *International Journal of Heat and Mass Transfer* 47 (2004) 135–147.
- [45] K. Pruess, J. Garcia, Multiphase flow dynamics during CO₂ injection into saline aquifers, *Environmental Geology* 42 (2002) 282–295.
- [46] A. Riaz, M. Hesse, H. Tchelepi, F. Orr, Onset of convection in a gravitationally unstable diffusive boundary layer in porous media, *Journal of Fluid Mechanics* 548 (2006) 87–111.
- [47] J. Rutqvist, D. Barr, J. Birkholzer, M. Chijimatsu, O. Kolditz, Q. Liu, Y. Oda, W. Wang, C. Zhang, Results from an international simulation study on coupled thermal, hydrological, and mechanical processes near geological nuclear waste repositories, *Journal of Nuclear Technology* 163 (2008) 101–109.
- [48] L. Sanavia, P. Pesavento, B.A. Schrefler, Finite element analysis of non-isothermal multiphase geomaterials with application to strain localization simulation, *Computational Mechanics* 37 (2006) 331–348.
- [49] A. Singh, U.-J. Görke, O. Kolditz, Numerical simulation of non-isothermal compositional gas flow: application to carbon dioxide injection into gas reservoirs, *Energy* 36 (2011) 3446–3458.
- [50] A. Singh, U.-J. Görke, O. Kolditz, Numerical analysis of thermal effects during carbon dioxide injection with enhanced gas recovery: a theoretical case study for the Altmark gas field, *Environmental Earth Sciences* 67 (2012), <http://dx.doi.org/10.1007/s12665-012-1689-9>.

- [51] A. Singh, P. Pilz, M. Zimmer, T. Kalbacher, U.-J. Görke, O. Kolditz, Numerical simulation of tracer transport in the altmark gas field, *Environmental Earth Sciences* 67 (2012), <http://dx.doi.org/10.1007/s12665-012-1688-x>.
- [52] G. Söderlind, Automatic control and adaptive time-stepping, *Numerical Algorithms* 31 (2002) 1–4.
- [53] R. Span, W. Wagner, A new equation of state for carbon dioxide covering the fluid region from the triple-point temperature to 1100 K at pressures up to 800 MPa, *Journal of Physical and Chemical Reference Data* 25 (1994) 1509–1596.
- [54] A. Truty, T. Zimmermann, Stabilized mixed finite element formulations for materially nonlinear partially saturated two-phase media, *Computer Methods in Applied Mechanics and Engineering* 195 (2006) 1517–1546.
- [55] C. Tsang, Coupled hydromechanical–thermochemical processes in rock fractures, *Reviews of Geophysics* 29 (1991) 537–551.
- [56] R. Walsh, C. McDermott, O. Kolditz, Numerical modeling of stress–permeability coupling in rough fractures, *Journal of Hydrogeology* 16 (2008) 613–627.
- [57] W. Wang, O. Kolditz, Object-oriented finite element analysis of thermo-hydro-mechanical (THM) problems in porous media, *International Journal of Numerical Methods in Engineering* 69 (2007) 162–201.
- [58] W. Wang, R. Rutqvist, U.-J. Gorke, J. Birkholzer, O. Kolditz, Non-isothermal flow in low permeable porous media: a comparison of Richards’ and two-phase flow approaches, *Environmental Earth Sciences* 62 (2011) 1197–1207.
- [59] W. Wang, T. Schnicke, O. Kolditz, Parallel finite element method and time stepping control for non-isothermal poro-elastic problems, *CMC – Computers Materials & Continua* 21 (2011) 217–235.
- [60] N. Watanabe, C. McDermott, W. Wang, T. Taniguchi, O. Kolditz, Uncertainty analysis of thermo-hydro-mechanical processes in heterogeneous porous media, *Computational Mechanics* 45 (2010) 263–280.